Insights into the collection and emplacement of granitic magma based on 3D seismic images of normal fault-related salt structures

D. G. Quirk*[1], R. S. D'Lemos, S. Mulligan[1] and B. M. R. Rabti

Geology, BMS, Oxford Brookes University, Gipsy Lane, Oxford OX3 0BP, UK

ABSTRACT

3D seismic data from salt structures in the Southern North Sea show how viscous fluids tend to migrate towards and flow upwards along the footwalls of active normal faults where zones of low stress are inherent. This process provides one potential solution for the question of how enough space is created to accommodate large granitic bodies in the crust. During episodes of regional extension, granitic melt may collect in the lower crust below normal detachments in domed areas from which magma may be sourced. Subsequently, in the upper crust, emplacement can occur in fault-bounded laccoliths at rates commensurate with other geological processes.

Terra Nova, 10, 268–273, 1998

Introduction

In recent years a growing body of research has supported models for the ascent of low-viscosity granitic magmas in narrow, fracture-bound conduits or dykes (Clemens and Mawer, 1992; Hutton, 1992; Petford *et al.*, 1994; Wada, 1994; Hanson and Glazner, 1995; McCaffrey and Petford, 1997). However, even in the light of this work, mechanisms for the collection and segregation of melt in the source region, its escape from the source region and the creation of space at the site of emplacement at rates consistent with the supply of magma are still a matter for speculation (e.g. Paterson and Fowler, 1993; Rubin, 1995). Also, many granite plutons do not simply conform with the dyke model, either because the original magma was apparently too viscous or because geophysical and geochemical data suggest that they are stock-shaped rather than constructed from or underlain by sheet-like bodies (Kukowski and Neugebauer, 1990; Paterson and Vernon, 1995; Weinberg, 1996). Part of the problem arises from the difficulty in assessing the three dimensional structure of the source region or the site of emplacement and understanding how granitic bodies evolved over time. Attempts have been made to address this by studying areas of tilted crust where granitoids frozen at various crustal levels are exposed in cross-section (e.g. D'Lemos *et al.*, 1992; Brown, 1994; Scaillet *et al.*, 1995). However, these give only a two dimensional view. In contrast, recent advances in the acquisition and processing of seismic data have provided detailed high-quality 3D images of salt bodies and their associated faults.

When researchers first looked to an explanation for the ascent of granite magmas, salt diapirs were considered useful analogues because they represent relatively large, rounded bodies of viscous fluid which have ascended from depth. Theoretical, experimental and field studies now show that buoyancy-driven magmatic diapirism is greatly limited by the rheology of the country rock and the rate of heat loss from the magma (e.g. Weinberg, 1996). Ironically, there is now also a growing realization that salt itself does not rise from depth as an active diapir because buoyancy forces are not sufficient to cause piercement of a thick cover (Weijermars *et al.*, 1993). Instead, normal faults facilitate the formation of many salt structures (e.g. Vendeville and Jackson, 1992), including the examples reported here. Despite differences in the rheology of salt and granite magma, the apparent similarities between the shapes of these salt structures and granitic bodies suggest that it is once more worth comparing these two systems.

Comparison of salt with granite

Salt and granitic magma share certain affinities. They are viscous fluids with negligible yield strength and a tendency to flow upwards through the crust (e.g. Jackson and Talbot, 1986; Clemens and Mawer, 1992). Both granitic plutons and salt structures are usually elliptical in plan view, commonly displaying contact-parallel marginal fabrics, with steep sides which are grossly discordant with surrounding country rocks (e.g. Talbot and Jackson, 1987; Paterson and Vernon, 1995). Also many granitic plutons and salt structures demonstrate close spatial and temporal associations with major faults (e.g. Atherton, 1993; Nalpas and Brun, 1993).

However, there are obvious key differences between salt and granite. Unlike salt, the rheology of magma is critically dependent on temperature. Although a partially molten granitic source region is likely to have a similar viscosity to salt (10^{16}–10^{19}Pa s), a segregated silicic melt will have a much lower viscosity (possibly 10^{4}–10^{10} Pa s) and a cooling, subliquidus granitic magma containing growing crystals and some source residue will have a viscosity between the two (Shaw, 1965; Arzi, 1978; Jackson and Talbot, 1986; Urai *et al.*, 1986; Talbot and Jackson, 1987; Wickham, 1987; Cruden, 1990; Emerman and Marrett, 1990; Kukowski and Neugebauer, 1990; Vendeville and Jackson, 1992; Van Keken *et al.*, 1993; Petford *et al.*, 1994; Dingwell *et al.*, 1996; Holtz *et al.*, 1996; Scaillet *et al.*, 1997). In contrast to granite, salt remains fluid in the subsurface and can flow during more than one tectonic episode. Other differences include the volumetric size of granitic intrusions, which are commonly an order of magnitude greater than salt structures, and the likely total ascent distances of salt (rarely more than 10 km) compared to that of mid-upper crustal granites (10–> 30 km).

We now go on to describe empirical evidence from 3D images of salt for the reaction of any viscous fluid to normal faulting. While accepting the gross differences between salt and granite, this

*Correspondence: Fax: +44/1865 483926; E-mail: dquirk@br-inc.com
[1]Present address: Burlington Resources (Irish Sea) Ltd, One Canada Square, Canary Wharf, London E14 5AA, UK.

process may have relevance to the collection and emplacement of high-viscosity magma during extension. Although salt structures and granite plutons also develop in compressive and strike-slip settings, these are not considered in this paper.

Salt structures formed during extension

The Southern North Sea is ideal for studying halokinesis (salt tectonics) because it contains a thick section of Zechstein (Late Permian) salt which is routinely drilled through and is imaged exceptionally well on modern seismic data. As is typical in most salt basins, halokinesis has been episodic and relates to distinct periods of tectonism in the late Jurassic, Late Cretaceous and early Miocene (Nalpas and Brun, 1993; Quirk, 1993). The majority of salt structures consists of elongate swells (or rollers) and walls of salt that are linked directly to major normal faults in the cover rocks (Fig. 1). Tilted blocks of Triassic strata are preserved to the sides of salt structures where the salt has thinned. The youngest normal faults occur directly above each structure and detach down one side of the salt so that the swell or wall is overlain by a half-graben or graben containing Triassic, Cretaceous and Tertiary strata. The salt forms domes in the footwalls of these normal faults (Fig. 1).

One of the largest salt structures in the Southern North Sea is shown on a recent high-quality 3D seismic data set in Fig. 2. The main structure consists of a NNW–SSE-trending wall of salt ≈ 30 km long, 1.5–2.5 km high and 0.7–1.5 km wide. In plan view the salt has a left-stepping, *en echelon* appearance linked directly to a parallel set of normal faults in the cover which vary in strike from NW–SE to N–S (Fig. 2a). The salt wall is underlain by a NNW–SSE fault zone which forms part of a regional-scale basement lineament. Detailed 3D seismic interpretation was carried out and tied to eight wells so that, by careful reference to chronostratigraphic thicknesses, structural geometries and regional information, the kinematic history of the salt structure could be determined. Originally an estimated 1400 m of Zechstein salt was deposited in the area followed by at least 1200 m of uniform Triassic strata. Halokinesis began in the Jurassic when E–W extension resulted in the formation of a set of N–S normal faults in the cover which detached along the top of the salt. Slip on these faults caused the Triassic strata to tilt while salt thinned below the hanging wall and thickened below the footwall adjacent to each fault (e.g. Figure 1a). Jurassic tectonism was followed by thermal subsidence and deposition of almost 3 km of Cretaceous and Tertiary sediment. Two further episodes of salt movement are recorded during this period. In the late Cretaceous new counter-dipping, NW–SE-trending normal fault detachments developed above the salt swells allowing them to grow upwards and extend laterally to produce a continuous salt wall (Fig. 2b), with relict swells forming spurs to the main wall, parallel to the older N–S faults (Fig. 2a). During the early Miocene renewed normal faulting and salt movement occurred. Biostratigraphic data below and above an unconformity formed at this time suggest that the crest of the structure rose ≈ 500 m in less than 200 000 years (> 2.5 km Myr^{-1}).

The explanation for the close relationship between normal faults and the growth of this and other salt structures is due to the mechanical behaviour of viscous fluids during crustal extension. Other viscous fluids such as granitic magma may react in a similar way as explained below.

Extensional footwall growth

Viscous fluids behave hydrodynamically in that they migrate towards regions of lower pressure where, impeded by the weight and strength of the cover rocks, they tend to collect causing doming (Jackson and Talbot, 1986). Fluid pressure comes from lithostatic stress (loading) and does not depend on buoyancy. A simple way of generating regions of lower pressure is with a normal fault in the cover rocks (e.g. Vendeville and Jackson, 1992). The fault cannot propagate in the fluid and it therefore detaches at the fluid boundary. As the fault slips a low-stress zone is created in the footwall directly below the fault as part of the overburden load is decoupled and transferred to the hanging wall. Fault block rotation also causes additional overburden weight to be transferred in a down-dip direction, away from the footwall and towards the hanging wall. The difference in stress between the footwall and the hanging wall is enhanced if erosion occurs on the up-thrown side of the fault or deposition occurs on the down-thrown side but it is not essential that this occurs. Again, although not a requirement, in low density fluids, additional buoyancy forces may be present if differences in height exist along the upper surface of the fluid. The fluid will react to the change in pressure so that it flows from underneath the hanging wall and up-dip along the footwall to collect in the low-stress zone below the fault (Fig. 1a). This process may be slow if the fluid is highly viscous but its effect is commonly observed in nature within over-pressured mudstones and evaporites and in sand-box experiments where low-viscosity silicone putty (e.g. 10^4–10^5Pa s) is used to model

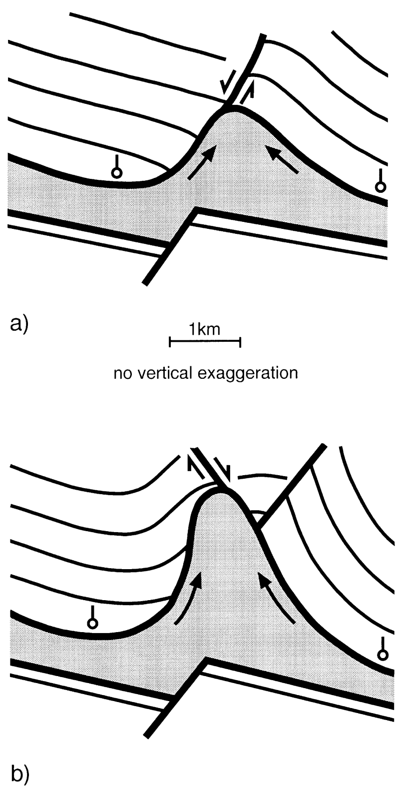

Fig. 1 Typical appearance of a salt swell (a) and a salt wall (b) observed on seismic sections from the Southern North Sea. The salt swell has a normal detachment on one side, the salt wall has a normal detachment on both sides although only one is active at any one time. Salt is shown in grey with inferred flow direction indicated by arrows; the inverted lollipop symbols indicate areas of excess lithostatic load.

geological phenomena (e.g. Weijermars *et al.*, 1993). It is here given the name extensional footwall growth and is to some degree self-perpetuating. As the volume of fluid increases below the fault, both the buoyancy stresses within the fluid and the area of fault lubricated by the fluid increase so that the amount of shear stress required to move the fault is reduced.

While the fluid continues to swell below the footwall, the cover rocks tilt away from the fault causing further unloading and deviatoric stresses to develop above the crest of the swell. These stresses may be relieved by gravitational sliding along a new fault dipping in a direction opposite to the original fault, which then ceases to move (e.g. Fig. 1b). The swell can then continue to enlarge by extensional footwall growth eventually forming a wall (Fig. 2b) similar to the model of reactive diapirism for salt proposed by Vendeville and Jackson (1992). As the relief of the swell or wall increases, buoyancy stress increases and lithostatic pressure above the structure decreases to the point where the yield strength of the cover may be exceeded, initiating active piercement. Alternatively, a vertical tension fracture may develop (Fig. 2b) forming a potential conduit for low-viscosity fluid.

Extensional footwall growth is limited mainly by the slip rate on the normal fault. The amount of footwall uplift recorded on major normal faults is typically in the range 2–6 km Myr^{-1} (e.g. Lister *et al.*, 1984; Hacker *et al.*,

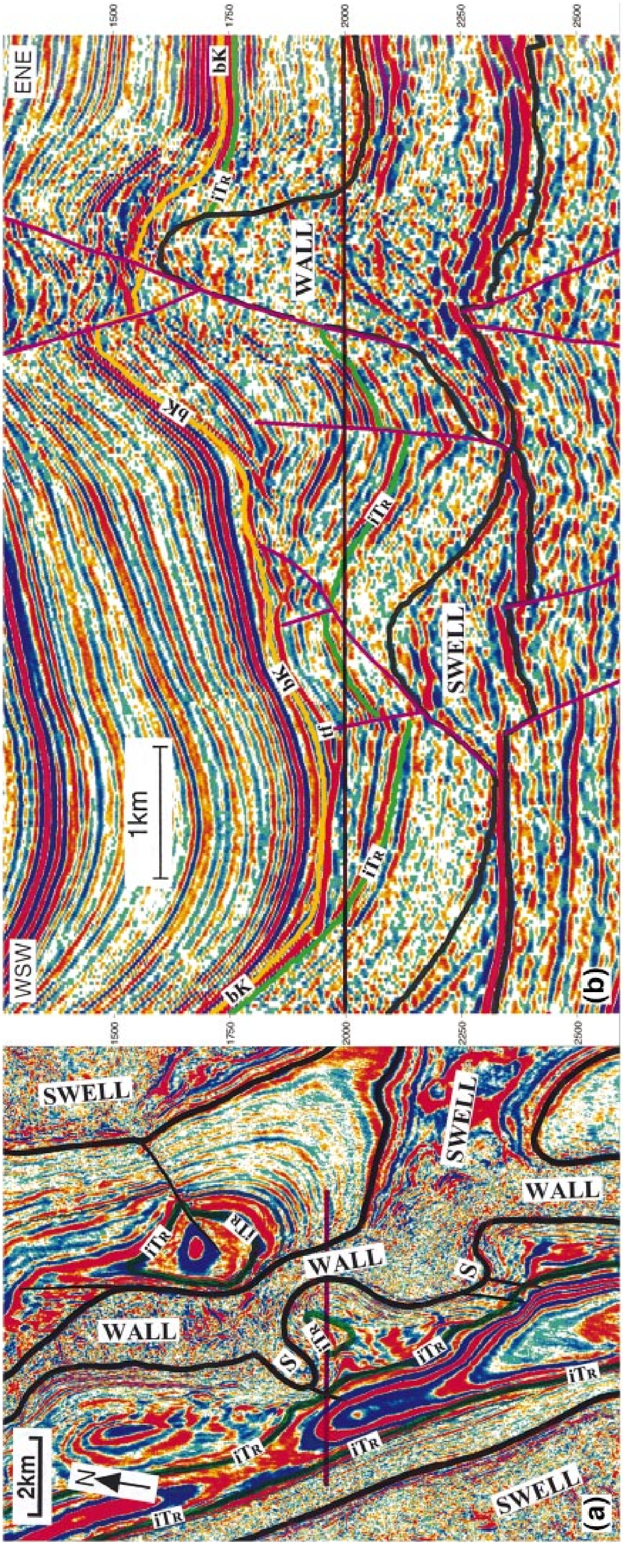

Fig. 2 (a) Horizontal time-slice at 2 s two way travel time across a 200-km^2 window in a large 3D seismic data set from the Southern North Sea. The boundary between Zechstein salt and the cover is outlined in black and an intra-Triassic horizon (iTR) is outlined in green. The position of the seismic line shown in (b) is marked with a straight line. S = small swell or spur. (b) 3D seismic section showing a salt swell and salt wall initiated during extension in the Jurassic. The top and base of the salt are outlined in black, an intra-Triassic horizon (iTR) in green, the base of the Cretaceous (bK) in yellow and faults are marked in magenta. The position of the time-slice shown in (a) is marked with a straight line. The vertical scale is in milliseconds two way travel time (vertical field of view is ≈ 3 km). tf = possible tension fracture.

1990; Holm *et al.*, 1992). These rates are greater than diapiric salt piercement (1–2 km Myr^{-1}; Kukal, 1990) but compare well with measured rates of ascent of salt during extension (2–7 km Myr^{-1}: Frumkin, 1996; the present paper).

Extensional footwall growth will always occur where a viscous fluid with minimal yield strength is overlain by cover rocks undergoing normal faulting. It represents a potential mechanism for moving large volumes of viscous fluid upwards in the crust with no inherent space problem as fluid expansion is accommodated by normal offset and block tilting.

Speculative model for the rise of granitic magma during extension

Many examples exist of granitic intrusions emplaced during active regional extension (e.g. Hutton, 1992; Petford and Atherton, 1992; Hanson and Glazner, 1995; Scaillet *et al.*, 1995). Upwelling asthenosphere provides a heat source (and possible mantle component) causing fertile lower crust to partially melt (Clemens and Mawer, 1992; Atherton, 1993; MacCready *et al.*, 1997) and behave as a fluid (Block and Royden, 1990) while the overlying crust is stretched and sheared (Wernicke, 1992). These are ideal conditions to initiate extensional footwall growth so that partially molten granitic source is likely to migrate up-dip into the footwalls of actively deforming normal fault blocks, collecting below where the faults detach (Stage 1, Fig. 3). As the crust thins by extension, lithostatic pressure decreases, particularly in upthrown blocks, and the temperature of the lower crust increases to cause further melting. Large volumes of melt could therefore pool under the footwalls of major detachment faults to form a domed region or swell.

In our model, as the swell continues to enlarge, the detachment is bent upwards so that deviatoric stress causes one of two things to happen. Either a counter-dipping normal detachment develops allowing the structure to enlarge as a granitic wall still attached to its source (cf. Fig. 1b) or, if the magma pressure overcomes the tensile strength of the cover rocks against which the swell is juxtaposed, active piercement or vertical fracturing takes place in the hanging wall (Stage 2, Fig. 3). In the latter case, where melt/source segregation can take place to produce relatively low-viscosity granitic magma, then this magma could ascend rapidly in dykes. While individual intrusions are likely to freeze rapidly, repeated injections could facilitate thermally sustainable ascent (Hanson and Glazner, 1995).

Upward migration continues until either a horizontal or shallow-dipping rheological boundary is encountered, such as a new detachment or ductile layer with potential for detachment, across which a fracture cannot propagate, or until vertical stress decreases below that of horizontal stress. At this shallower level the magma may be emplaced as a laccolith (e.g. Clemens and Mawer, 1992). Accommodation of the laccolith can also be by extensional footwall growth if normal faulting occurs along one side of the pluton so that the roof rises and tilts, with magma filling the expanding wedge (Stage 3, Fig. 3). By this means, thicker intrusive bodies may accumulate than would be predicted if uplift of the roof was driven by magma pressure alone (McCaffrey and Petford, 1997) and emplacement is not dependent on low viscosity (see Emerman and Marrett, 1990). As the body grows, normal detachments may switch from one side of the pluton to the other, much as happens during ascent of a salt wall (Fig. 1b). Each detachment occurs at the cover/fluid interface and is therefore thin provided the temperature of the magma remains above its solidus. If the detachment ceases to move it may then become overprinted by intrusive processes such as stoping and ballooning. Alternatively, if the carapace of the magma solidifies, the effects of normal faulting may work inwards to form a sheared margin. The pluton will cease to enlarge if the source of magma is cut off, or if it cools to a point where it will no longer flow, or if magma pressure decreases to that of the confining stress, or if normal faulting ceases.

Granite structures predicted from the model

Our model leads to certain predictions. While none of the features are exclusive to the model, taken in combination they could indicate whether extensional footwall growth is a valid mechanism for the sourcing or the emplacement of certain types of granitic bodies. In lower crustal sections, there should be evidence for wholesale flow of granitic source regions up-dip towards inclined normal detachments. Melt and restite will have collected in domal areas beneath the detachments where magma may have segregated, possibly due to pressure release caused by slip on the detachment (Stage 1, Fig. 3). Extensional dykes may also be present. Features similar to those predicted are observed in basin and range-type extensional settings where dome-like metamorphic core complexes have been carried to surface from depths of > 15 km in the footwalls of low-angle normal detachments (e.g. Hacker *et al.*, 1990). Examples where segregation of granitic melt has occurred include the Naxos metamorphic core complex, Greece (Lister *et al.*, 1984); the Black

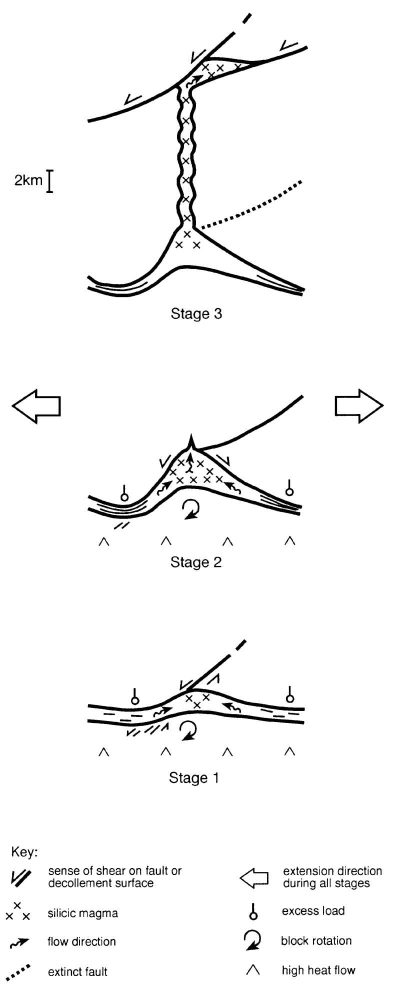

Fig. 3 Schematic cross-sections showing model for collection, ascent and emplacement of granitic magma during crustal-scale extensional shearing. See text for discussion of the three stages.

Mountains magmatic complex, California (Holm *et al.*, 1992); the D'Entrecasteaux Islands core complexes, Papua New Guinea (Hill *et al.*, 1992); the Kigluaik gneiss dome, Alaska (Amato *et al.*, 1994); and the Ruby Mountains core complex, Nevada (MacCready *et al.*, 1997).

After collection and segregation, ascent of granitic magma is probably via subvertical feeders, either as narrow dykes (low-viscosity magma) or as wider, fault-bound conduits (high-viscosity magma). These may become inclined due to fault block rotation if normal slip on the detachment continues over a period of time.

The feeders may open up into elongate, fault-bound wedge- or dome-shaped plutons at higher structural levels (Stage 3, Fig. 3). Good evidence of this would be the occurrence of a syn-intrusion normal fault or shear zone bounding and extending away from the pluton, parallel to its direction of elongation. However, since slip can occur within the outer margin of the magma body itself, at certain levels of exposure there need be no direct indication of a fault plane and shear fabrics may become overprinted by subsequent magmatic and tectonic processes (e.g. stoping, ballooning, recrystallization, solid state deformation). If normal fault movement continues after the granite has been emplaced, the solidifying pluton will be rapidly exhumed due to footwall uplift. It may thus end up juxtaposed against a half-graben in its hanging wall and serve as a source of local sediment.

Examples of granitic intrusions which appear to have been emplaced during extension on the footwall side of active normal faults, as predicted, include the Cordillera Blanca batholith in Peru (Petford and Atherton, 1992), the Mount Givens pluton, California (Tobisch *et al.*, 1993), granitic plutons on the Great Escarpment in Yemen (Davison *et al.*, 1994), the Gangotri granite in the High Himalaya (Scaillet *et al.*, 1995), the Los Pedroches batholith, Spain (Aranguren *et al.*, 1997), and the Leinster granite, Ireland (S. Mulligan, unpubl. data). Depending on the rate of fault movement, a granitic body 6 km thick could be emplaced in as little as 1 Myr.

Conclusions

3D analysis of salt structures provides insights into how large volumes of upwards-flowing viscous fluid (salt) can be accommodated in the crust in reaction to changes, in pressure caused by normal faulting. While bearing in mind the obvious differences between salt and granitic magma, we consider that a similar process may help explain the collection and emplacement of certain granitic magmas. Lateral flow and doming of source regions may occur in the footwalls of inclined detachments as a result of high heat flow and fault block rotation. These domal areas may act as sites for melt segregation and as seed points for the ascent of magma within fracture-bound conduits to upper crustal levels. The magma can accumulate in large volumes in low-stress regions below major normal faults forming wedge- or dome-shaped laccoliths. Granitic complexes exist which exhibit the characteristics predicted from this mechanism suggesting that analogies with extension-related salt structures have some validity.

Acknowledgements

We thank Fina Petroleum and block 44/29 partners for permission to use their 3D seismic data. Sponsorship for part of the research came from Zueitina Oil and Schlumberger GeoQuest. We are grateful for advice and reviews from A. Brandon, M. Jackson, A. Glazner, R. Kerr and help from L. Hill.

References

Amato, J.M., Wright, J.E., Gans, P.B. and Miller, E.L., 1994. Magmatically induced metamorphism and deformation in the Kigluaik gneiss dome, Seward Peninsula, Alaska. *Tectonics*, **13**, 515–527.

Aranguren, A., Larrea, F., Carracedo, M., Cuevas, J. and Tubía, J.M., 1997. The Los Pedroches Batholith (Southern Spain): polyphase interplay between shear zones in transtension and setting of granites. In: *Granite: from Segregation of Melt to Emplacement Fabrics* (J.L. Bouchez, D.H.W. Hutton and W.E. Stephens, eds), pp. 215–230. Kluwer, Dordrecht.

Arzi, A.A., 1978. Critical phenomena in the rheology of partially melted rocks. *Tectonophysics*, **44**, 173–184.

Atherton, M.P., 1993. Granite magmatism. *J. Geol. Soc. London*, **150**, 1009–1023.

Block, L. and Royden, L.H., 1990. Core complex geometries and regional scale flow in the lower crust. *Tectonics*, **9**, 557–567.

Brown, M., 1994. The generation, segregation, ascent and emplacement of granite magma: the migmatite-to-crustally-derived granite connection in thickened orogens. *Earth Sci. Rev.*, **36**, 83–130.

Clemens, J.D. and Mawer, C.K., 1992. Granitic magma transport by fracture propagation. *Tectonophysics*, **204**, 339–360.

Cruden, A.R., 1990. Flow and fabric development during the diapiric rise of magma. *J. Geol.*, **98**, 681–698.

D'Lemos, R.S., Brown, M. and Strachan, R.A., 1992. Granite generation, ascent and emplacement within a transpressional orogen. *J. Geol. Soc., London*, **149**, 487–490.

Davison, I., Al-Kadasi, M., Al-Khirbash, S. *et al.*, 1994. Geological evolution of the southeastern Red Sea Rift margin, Republic of Yemen. *Bull. Geol. Soc. Am.*, **106**, 1474–1493.

Dingwell, D.B., Hess, K.-U. and Knoche, R., 1996. Granite and granitic pegmatite melts: volumes and viscosities. *Trans. R. Soc. Edinb.: Earth Sci.*, **87**, 65–72.

Emerman, S.H. and Marrett, R., 1990. Why dikes? *Geology*, **18**, 231–233.

Frumkin, A., 1996. Uplift rate relative to base-levels of a salt diapir (Dead Sea Basin, Israel) as indicated by cave levels. In: *Salt Tectonics* (G.I. Alsop, D.J. Blundell and I. Davison, eds). *Spec. Publ. Geol. Soc. London*, **100**, 41–47

Hacker, B.R., Yin, A., Christie, J.M. and Snoke, A.W., 1990. Differential stress, strain rate and temperatures of mylonitization in the Ruby Mountains, Nevada: implications for the rate and duration of uplift. *J. Geophys. Res.*, **95**, 8569–8580.

Hanson, R.B. and Glazner, A.F., 1995. Thermal requirements for extensional emplacement of granitoids. *Geology*, **23**, 213–216.

Hill, E.J., Baldwin, S.L. and Lister, G.S., 1992. Unroofing of active metamorphic core complexes in the D'Entrecasteaux Islands, Papua New Guinea. *Geology*, **20**, 907–910.

Holm, D.K., Snow, J.K. and Lux, D.R., 1992. Thermal and barometric constraints on the intrusive and unroofing history of the Black Mountains: implications for timing, initial dip, and kinematics of detachment faulting in the Death Valley region, California. *Tectonics*, **11**, 507–522.

Holtz, F., Scaillet, B., Behrens, H., Schulze, F. and Pichavant, M., 1996. Water contents of felsic melts: application to the rheological properties of granitic magmas. *Trans. R. Soc. Edinb.: Earth Sci.*, **87**, 57–64.

Hutton, D.H.W., 1992. Granite sheeted complexes: evidence for the dyking ascent mechanism. *Trans. R. Soc. Edinb.: Earth Sci.*, **83**, 377–382.

Jackson, M.P.A. and Talbot, C.J., 1986. External shapes, strain rates, and dynamics of salt structures. *Geol Soc. Am. Bull.*, **97**, 305–323.

Kukal, Z., 1990. The rate of geological processes. *Earth Sci. Revs*, **29**, 265.

Kukowski, N. and Neugebauer, H.J., 1990. On the ascent and emplacement of granitoid magma bodies–dynamic-thermal numerical models. *Geol. Rndsch.*, **79**, 227–239.

Lister, G.S., Banga, G. and Feenstra, A., 1984. Metamorphic core complexes of Cordilleran type in the Cyclades, Aegean Sea, Greece. *Geology*, **12**, 221–225.

MacCready, T., Snoke, A.W., Wright, J.E. and Howard, K.A., 1997. Mid-crustal flow during Tertiary extension in the Ruby Mountains core complex, Nevada. *Bull. Geol. Soc. Am.*, **109**, 1576–1594.

McCaffrey, K.J.W. and Petford, N., 1997. Are granitic intrusions scale invariant? *J. Geol. Soc. London*, **154**, 1–4.

Nalpas, T. and Brun, J.-P., 1993. Salt flow and diapirism related to extension at crustal scale. *Tectonophysics*, **228**, 349–362.

Paterson, S.R. and Fowler, T.K. Jr, 1993. Re-examining pluton emplacement processes. *J. Struct. Geol.*, **15**, 191–206.

Paterson, S.R. and Vernon, R.H., 1995. Bursting the bubble of ballooning plutons: a return to nested diapirs emplaced by multiple processes. *Bull. Geol. Soc. Am.*, **107**, 1356–1380.

Petford, N. and Atherton, M.P., 1992. Granitoid emplacement and deformation along a major crustal lineament: the Cordillera Blanca, Peru. *Tectonophysics*, **205**, 171–185.

Petford, N., Lister, J.R. and Kerr, R.C., 1994. The ascent of felsic magmas in dykes. *Lithos*, **32**, 161–168.

Quirk, D.G., 1993. Interpreting the Upper Carboniferous of the Dutch Cleaver Bank High. In: *Petroleum Geology of Northwest Europe: Proceedings of the 4th Conference* (J.R. Parker, ed.), pp. 697–706. Geological Society, London.

Rubin, A.M., 1995. Getting granite dikes out of the source region. *J. Geophys. Res.*, **100**, 5911–5929.

Scaillet, B., Holtz, F. and Pichavant, M., 1997. Rheological properties of granitic magmas in their crystallisation range. In: *Granite: from Segregation of Melt to Emplacement Fabrics* (J.L. Bouchez, D.H.W. Hutton and W.E. Stephens, eds), pp. 11–29. Kluwer, Dordrecht.

Scaillet, B., Pêcher, A., Rochette, P. and Champenois, M., 1995. The Gangotri granite (Garwhal Himalaya): laccolithic emplacement in an extending collisional belt. *J. Geophys. Res.*, **100**, 585–607.

Shaw, H.R., 1965. Comments on viscosity, crystal settling and convection in granitic magmas. *Am. J. Sci.*, **263**, 120–152.

Talbot, C.J. and Jackson, M.P.A., 1987. Internal kinematics of salt diapirs. *Bull. Am. Ass. Petrol. Geol.*, **71**, 1068–1093.

Tobisch, O.T., Renne, P.R. and Saleeby, J.B., 1993. Deformation resulting from regional extension during pluton ascent and emplacement, central Sierra Nevada, California. *J. Struct. Geol*, **15**, 609–628.

Urai, J.L., Spiers, C.J., Zwart, H.J. and Lister, G.S., 1986. Weakening of rock salt by water during long-term creep. *Nature*, **324**, 554–557.

Van Keken, P.E., Spiers, C.J., van den Berg, A.P. and Muyzert, E.J., 1993. The effective viscosity of rocksalt: implementation of steady-state creep laws in numerical models of salt diapirism. *Tectonophysics*, **225**, 457–476.

Vendeville, B.C. and Jackson, M.P.A., 1992. The rise of diapirs during thin-skinned extension. *Mar. Petrol. Geol.*, **9**, 331–353.

Wada, Y., 1994. On the relationship between dyke width and magma viscosity. *J. Geophys. Res.*, **99**, 17743–17755.

Weijermars, R., Jackson, M.P.A. and Vendeville, B.C., 1993. Rheological and tectonic modelling of salt provinces. *Tectonophysics*, **217**, 143–174.

Weinberg, R.F., 1996. Ascent mechanism of felsic magmas: news and views. *Trans. R. Soc. Edinb.: Earth Sci.*, **87**, 95–103.

Wernicke, B., 1992. Cenozoic extensional tectonics of the U.S. Cordillera. In: *The Geology of North America — the Cordilleran Orogen: Conterminous U.S.* (B.C. Burchfiel, P.W. Lipman and M.L. Zoback, eds), G-3, pp. 553–581. Geological Society of America, Boulder, CO.

Wickham, S.M., 1987. The segregation and emplacement of granitic magmas. *J. Geol Soc. London*, **144**, 281–297.

Received 22 July 1998; revised version accepted 12 February 1999